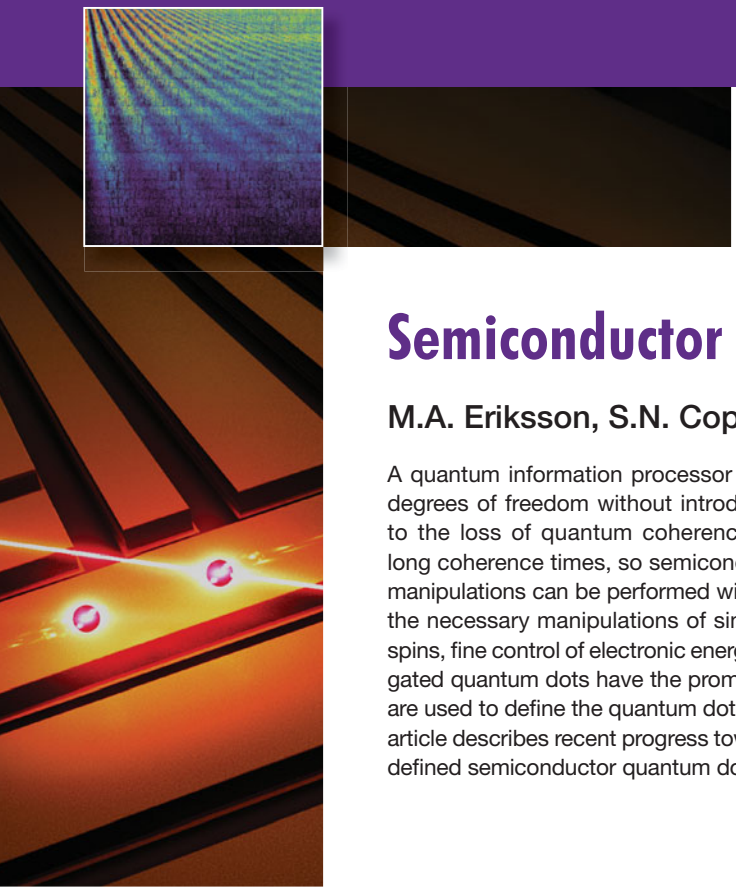


Semiconductor quantum dot qubits

M.A. Eriksson, S.N. Coppersmith, and M.G. Lagally

A quantum information processor must perform accurate manipulations of many quantum degrees of freedom without introducing strong interactions with the environment that lead to the loss of quantum coherence. Spins in semiconductors have been shown to have long coherence times, so semiconducting quantum processors are feasible if the necessary manipulations can be performed without introducing excessive spin decoherence. To perform the necessary manipulations of single spins and to control the couplings between different spins, fine control of electronic energy levels and wave function overlaps is required. Electrically gated quantum dots have the promise of enabling such control, because the same gates that are used to define the quantum dot can be used to perform the necessary manipulations. This article describes recent progress toward the development of high-fidelity qubits using top-gate defined semiconductor quantum dots.

Introduction

The goal of developing a large-scale quantum information processor has attracted much interest and activity over the past decade, not just because quantum information processors have the potential to efficiently solve problems that are not tractable using classical computers,[1] but also because substantial fundamental physics and materials science questions must be understood in order to fabricate such a device.

To understand how large a quantum computer needs to be in order for it to be potentially much more powerful than a classical one, it is useful to compare the number of quantities needed to describe a physical state classically and quantum-mechanically.[2] For a system with M classical degrees of freedom, the size of the quantum mechanical description grows exponentially with M. A quantum computer with N qubits has the potential to outperform a current classical computer with M transistors only when $N > \log_2 M$. For $M = 10^9$, typical of a personal computer, one needs $N > 30$. Therefore, the current state of the art of 15 qubits achieved in ion traps,[3] though extremely impressive, does not yet improve upon classical computers from a purely computational point of view. Practically useful quantum computational devices will require at least hundreds and probably thousands of qubits.[4] Therefore, a feasible path to scalability is an important criterion for the development of quantum information processing devices.

In 1998, Loss and DiVincenzo proposed to use electron spins in quantum dots formed in quantum wells as qubits, through the use of electrostatic fields generated by surface gates.[5] Constructing qubits using such electrically gated quantum dots has attracted substantial interest and effort, both theoretical[6–11] and experimental.[12–17] While fabrication of gated quantum dots with few-electron occupancy is demanding, this strategy has the important advantage that the metal top gates that are used to define the quantum dots can also be used to perform the necessary manipulations.[18] Control of the interactions between dots is possible simply by changing voltages on the electrostatic gates and is greatly facilitated by the relatively large spatial extent of electron wave functions in semiconductor dots. Because of the similarities with classical electronics, it is plausible that both scale-up and integration with classical electronics will be feasible. However, first it is necessary to construct the basic building blocks of a quantum computer: controllable single qubits and high-fidelity two-qubit gates. Quantum dot-based single qubits have been demonstrated in both III–V and Group IV materials systems,[12,15,17,19,20] while two-qubit gates have been demonstrated in gallium arsenide devices.[16,21] However, further improvements to the fidelity of both the single and two-qubit gates are required to achieve the performance necessary for implementation of a scalable quantum processor.[4]

This article discusses the materials science and engineering underlying the development of quantum dot qubits. The main focus is on quantum dots made using top gates on

M.A. Eriksson, Department of Physics, University of Wisconsin–Madison; maeriksson@wisc.edu
S.N. Coppersmith, Department of Physics, University of Wisconsin–Madison; snc@physics.wisc.edu
M.G. Lagally, Department of Materials Science and Engineering, University of Wisconsin–Madison; lagally@engr.wisc.edu
DOI: 10.1557/mrs.2013.208

© 2013 Materials Research Society
https://doi.org/10.1557/mrs.2013.208 Published online by Cambridge University Press

heterostructures of GaAs/AlGaAs or Si/SiGe as well as on silicon metal-oxide-semiconductor (MOS) structures. All of these materials serve as hosts for quantum dots in which the electron wave functions extend over lengths on the order of tens of nanometers. Several groups are pursuing device strategies involving electronic wave functions bound to donors, which have spatial extents $\lesssim$5 nm.[22–24] Such devices can be viewed as being implementations of defect-based quantum computing (see article by Gordon et al. in this issue), but the physical principles and fabrication techniques have many commonalities with quantum dot qubits; these relationships in silicon devices have been reviewed recently.[25]

First, we discuss general considerations common to gated quantum dots formed in heterostructures, methods of measuring both charge and spin, and the achievement of few- (and one-) electron occupation of quantum dots. Second, we discuss approaches to implementing quantum gates and some of the relative advantages and disadvantages of the two most common material hosts for the electron wave function, GaAs and Si. The **sidebar** discusses some of the special approaches that are required for heterostructure growth in the Si/SiGe materials system. Finally, we discuss current work that aims to enhance the fidelity of qubit operations and measurements.

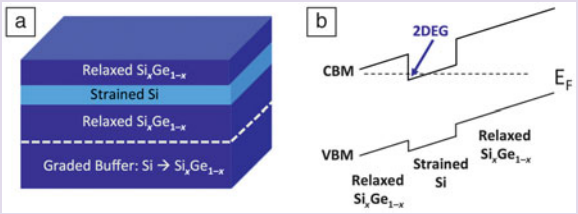
Electrically gated quantum dot qubits: General considerations

A qubit is a system with two energy levels. The prototypical candidate for such a system is the single electron, which has two spin states ($S_z = \hbar/2$ and $S_z = -\hbar/2$). In such a spin qubit, the electron's physical location is fixed inside a single semiconductor quantum dot, and qubit manipulation focuses solely on rotation of the electron spin. Alternatively, a qubit can be the physical position itself of an electron in a double quantum dot. In this case, spin is ignored, and the two qubit states consist of the electron occupying the left or the right quantum dot. Because spin couples weakly to other objects, the single-spin qubit has both relatively slow decoherence and slow manipulation, while the charge qubit is both fast to manipulate and fast to decohere. We return later to this set of trade-offs, which have led to very interesting proposals and implementations of qubits consisting of two and even three electrons.

Fabrication of Si/SiGe heterostructures for defining Si quantum dots

Strained-silicon/relaxed silicon-germanium alloy (strained-Si/Si_xGe_{1-x}) heterostructures are a foundation of Group IV-element quantum dot-based quantum electronics and quantum computation. In bulk, unstrained Si and Ge, the conduction-band minimum is located along high-symmetry directions away from the zone center, so that states for electrons in bulk, unstrained Si and Ge are multiply degenerate.[28] For quantum electronics, the ability to lift this degeneracy with strain is particularly important. Strain breaks the crystallographic symmetry in materials, leading to, among other effects, changes in the electronic band structure that reduce the conduction-band degeneracy. The formation of single-electron quantum dot devices in Si-based systems requires a very thin layer of tensilely strained Si, epitaxially grown, and confined between Si_xGe_{1-x} layers. The Si layer is tensilely strained because the lattice constant of Si_xGe_{1-x} is larger than that of Si. A two-dimensional electron gas (2DEG) is created in the strained-Si layer (see Figure), and this quantum confinement fully removes the conduction band degeneracy. A series of lateral gates, when biased properly, can be used to confine individual electrons in quantum dots.

To create a quantum well in the Si layer, so that the states of the conduction-band minimum are sufficiently separated to isolate only one sub-band below the Fermi level, requires specific compositions in the fully relaxed Si_xGe_{1-x} layers (30% Ge is common in present-day devices, but lower percentages are possible) and specific thicknesses of the strained-Si layer (~10 nm). The traditional approach to achieving relaxed Si_xGe_{1-x} alloy substrates involves growing step-graded, thick buffer layers onto Si (001) substrates.[27] The resulting films are relaxed through the formation of misfit dislocations with very few threading dislocations propagating vertically through the near surface, active regions of the heterostructure. More recent work has shown that completely releasing membranes of Si_xGe_{1-x} grown on silicon-on-insulator can lead to very high-quality relaxed Si_xGe_{1-x} films that can then be deposited on a wide variety of other materials, leading to opportunities for ultra-low dislocation densities and heterogeneous integration.[79,80]



(a) Schematic diagram of the physical film structure. A relaxed SiGe buffer layer strains a thin Si layer that will form a quantum well for electrons. (b) Schematic diagram of the band offsets for strained-Si/SiGe heterostructures, resulting in a two-dimensional electron gas (2DEG) in the strained-Si quantum well. The electron density in the quantum well will depend on the position and density of a dopant layer or on the voltage applied to a metallic gate on the surface, resulting in a density-dependent band bending below the quantum well (not shown). CBM, conduction-band minimum; VBM, valence-band minimum.

https://doi.org/10.1557/mrs.2013.208 Published online by Cambridge University Press

Gated quantum dots in semiconductor heterostructures make excellent hosts for qubits formed from small numbers of electrons, and many of the materials and design considerations are common to both III–V and Group IV materials. Because electrostatic fields alone cannot confine electrons in three dimensions, a change in material composition is universally used to confine electrons in at least one direction. **Figure 1**a shows the canonical design: the carriers in GaAs/AlGaAs devices are typically introduced by modulation doping in the AlGaAs layer near the surface.[26] $Al_xGa_{1-x}As$ has virtually the same lattice constant for all values of x, so knowledge of x as a function of depth fully describes the structure. Because electrons have higher affinity in GaAs than in AlGaAs, they have lower energy in the underlying GaAs layer, and they are pinned against the GaAs/AlGaAs interface by their attraction to the positively charged ionized donors above them, forming a mobile two-dimensional electron gas. Metallic top gates are used to deplete electrons and define the quantum dot, as indicated schematically in Figure 1a.

Because Ge is a larger atom than Si, Si_xGe_{1-x} has a natural lattice constant that increases by 4.2% from pure Si to pure Ge.[27] A description of a Si/Si_xGe_{1-x} heterostructure therefore must include both the composition x and the lattice constant, typically described by the composition at which the relaxed lattice constant matches that of the heterostructure. As described in the sidebar, growing a thin Si layer on a relaxed Si_xGe_{1-x} layer results in a well that will attract and confine electrons.[28] As shown in Figure 1b, modulation doping will then produce a two-dimensional electron gas. An alternative approach shown in Figure 1c is to omit the modulation doping layer and instead accumulate electrons with an electrostatic gate positioned over the top of, and separated by oxide from, the electron gas.[29] Eliminating the modulation doping layer in this way reduces low-frequency charge noise known as "switching." Heterostructure and device designs are reviewed for GaAs in Reference 18 and for Si in Reference 25.

Charge measurement and achievement of few-electron occupation

Typically, experiments on quantum dots determine the charge occupations of all the dots in the device. Charge-sensing is

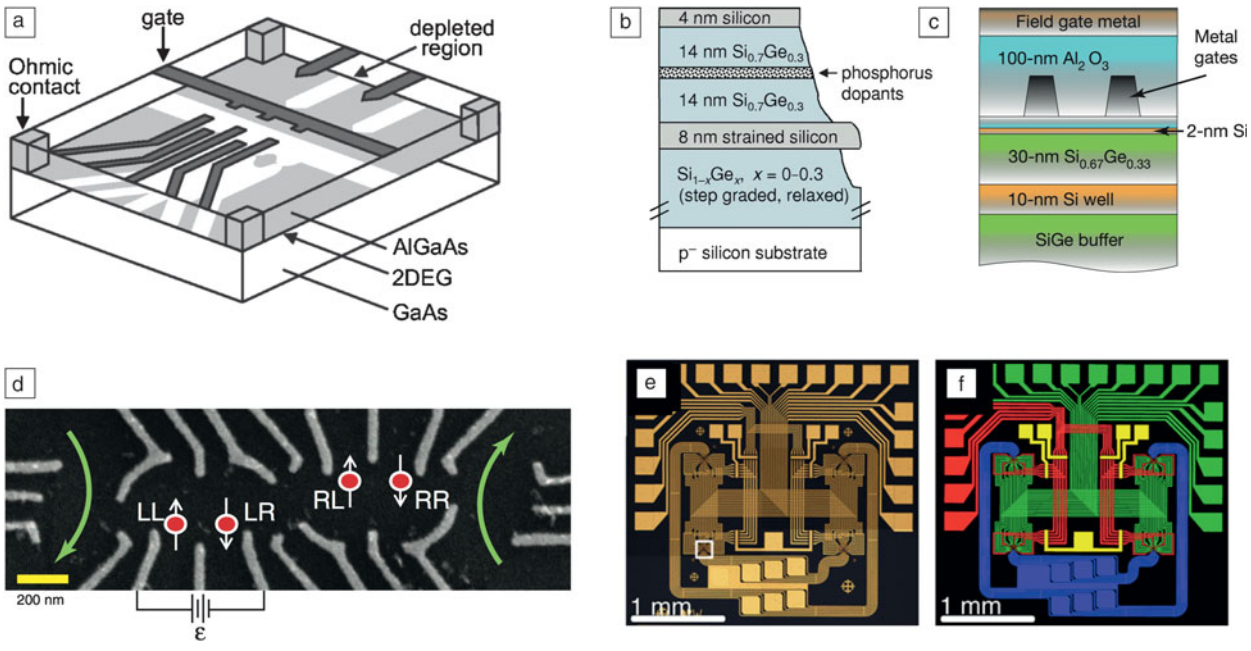


Figure 1. Semiconductor heterostructures and gate designs for gated quantum dots. (a) A two-dimensional electron gas (2DEG) is formed at the interface between an AlGaAs barrier and a GaAs layer. The electric field from ionized dopants pins the 2DEG against the upper interface. Reprinted with permission from Reference 18. © 2007 American Physical Society. (b) Formation of a 2DEG in Si/SiGe heterostructures requires that the Si layer be tensile-strained, which can be accomplished by growing the heterostructure on top of a relaxed SiGe buffer layer. Reprinted with permission from Reference 78. © 2006 American Institute of Physics. (c) By using a positively biased accumulation (or field) gate, electrons can be accumulated in a Si quantum well without the incorporation of a modulation-doping layer. Reprinted with permission from Reference 15. © 2012 Macmillan Publishers Ltd. (d) Gate design for a pair of coupled double quantum dots formed on a GaAs/AlGaAs heterostructure. LL (left qubit, left dot) and LR (left qubit, right dot) form one double-dot qubit, and RL (right qubit, left dot) and RR (right qubit, right dot) form a second such qubit. The capacitance between the two double dots enables two-qubit manipulation. Reprinted with permission from Reference 16. © 2012 American Association for the Advancement of Science. (e) Optical image of a multiplexed set of four double quantum dots. The white rectangle in the lower-left quadrant of the image shows the location of one double quantum dot. (f) Colorized version of the image shown in (e): Red indicates accumulation gates that are multiplexed by transistor switches shown in yellow; green indicates depletion gates that confine the electrons within the double quantum dots; and blue indicates high-frequency voltage lines for fast manipulation. (e–f) Reprinted with permission from Reference 43. © 2013 American Institute of Physics.

https://doi.org/10.1557/mrs.2013.208 Published online by Cambridge University Press

usually performed by measuring the current through nearby quantum point contacts[30,31] or auxiliary quantum dots.[16] Figure 1d shows two neighboring double quantum dots; the green arrows on the left and the right show the expected current path through charge sensing, auxiliary quantum dots. As is typically the case, a single charge sensor is sufficient to measure changes in charge occupation on both the left and the right sides of an individual double quantum dot.

While qubits formed in quantum dots can be more complicated than one-electron—both two- and three-electron qubits have been proposed and fabricated—essentially all qubit architectures make use of quantum dots with few-electron occupation.[32–35] Electrically gated quantum dots with single-electron occupancy were achieved in GaAs heterostructures in 2000[36] and in Si/SiGe heterostructures in 2007.[37] The key advances involve materials development to reduce inhomogeneities at the relevant interfaces and gate design to enable a reduction in the number of electrons in the dot without excessive suppression of the tunnel rates into and out of the dot. The maintenance of fast tunnel rates is critical for qubit operation and readout.[12,13,15,34,38]

An important figure of merit for charge-sensing measurements is the time required to resolve a one-electron change in the quantum dot occupation. Charge-sensing quantum point contacts can be measured using conventional current amplifiers, in which speed limitations are determined by the RC delay arising from the circuit impedance R (typically between 50 kΩ and 500 kΩ) and the capacitance C (which can be quite large, because the experiments are performed inside low-temperature cryostats with relatively long wiring paths). This limitation can be circumvented by using LC matching networks to enable radiofrequency reflection measurements of high-impedance charge sensors using 50-ohm transmission lines, resulting in much higher measurement bandwidth. This radiofrequency technique, first applied to superconducting circuits,[39] has been adapted to increase the measurement bandwidth for charge-sensing quantum point contacts coupled to semiconductor quantum dots.[40,41]

An advantage of qubits formed in semiconductors is the ability to use classical semiconductor devices (usually field-effect transistor-based circuits) at low temperatures in parallel (and even on the same chip) with quantum devices. CMOS comparators have been proposed for fast measurement of single-electron transistor-based charge sensors, with potential measurement times as short as 1 ns.[42] Semiconductor gated quantum dots themselves closely resemble field-effect transistors (albeit with many more gates per device), suggesting the possibility of true on-chip integration of classical and quantum devices. As shown in Figure 1e–f, unipolar transistors fabricated on-chip in an undoped Si/SiGe heterostructure have recently been used to integrate a multiplexing circuit for readout of quantum devices.[43] This strategy, demonstrated in Si devices, is expected to be effective in any semiconductor host.

Spin measurement

Although spin is difficult to measure directly, both single- and two-electron spin states can be measured with charge-sensing quantum point contacts using a method called spin-to-charge conversion.[44] A general approach to single-shot readout—readout of a quantum state without averaging over many measurements—is possible by making use of the energy difference between two spin states:[45] Quantum dot gate voltages are tuned such that the high-energy spin state can tunnel to a nearby reservoir (or to another dot), while the low-energy spin state is frozen in place (**Figure 2**a–b). Using this method, single-shot measurement of electron spins has shown T_1 spin relaxation times longer than 1 second in both GaAs/AlGaAs[46] and Si/SiGe quantum dots.[14]

Spin-to-charge conversion also can be used to determine whether two electrons are in a singlet or triplet state.[12,47] The influence of these two spin states on electron motion in quantum dots was first demonstrated in Pauli spin blockade measurements of transport through the dots themselves, rather than in charge sensing.[48] Starting with one electron in each dot—the (1,1) state—spin conservation plus the Pauli exclusion principle forbid simple tunneling of one electron to transition

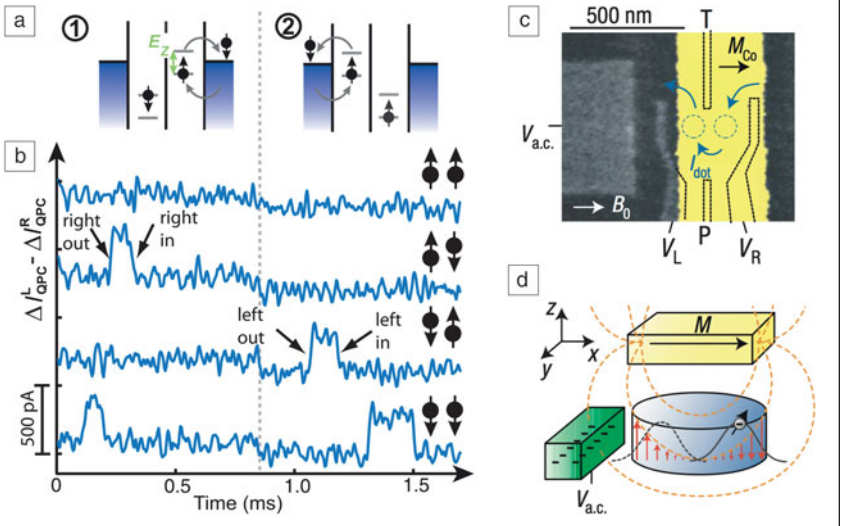


Figure 2. (a) Independent single-spin measurement process on both sides of a double quantum dot in GaAs. (1) A process in which a spin-down in the right dot tunnels out to the right lead, and a spin-up tunnels back into the dot. (2) The analogous process involving the left dot and the left lead. (b) Four example measurements showing the discrimination of up-up, up-down, down-up, and down-down states of single spins in two quantum dots. (a–b) Reprinted with permission from Reference 21. © 2011 American Association for the Advancement of Science. (c) Composite schematic diagram showing the position of a micromagnet (yellow) over the top of a GaAs quantum dot. (d) The fringing field of the micromagnet produces a magnetic field difference between the two quantum dots. (c–d) Reprinted with permission from Reference 20. © 2008 Macmillan Publishers Ltd.

https://doi.org/10.1557/mrs.2013.208 Published online by Cambridge University Press

from a triplet (1,1) state to the low-energy singlet (0,2) state. Transitions are allowed to the triplet (0,2) state, but accessing this state requires placing one of the electrons into an excited orbital so that the energy gap between the singlet and triplet (0,2) states can be very large, enabling robust discrimination between singlet and triplet states.

It was not initially clear that readout of singlet-triplet states would be possible in Si/SiGe quantum dots using this method, because tensile-strained silicon has a twofold degeneracy in the conduction band.[28] If not lifted, this degeneracy would destroy the Pauli spin blockade. Measurements of the quantum Hall effect in extended two-dimensional electron systems had shown very small splittings (less than 100 μeV) of the valley states at low magnetic fields.[49] It was shown that these small splittings were not intrinsic to the quantum well, but rather they arose from steps between atomic terraces at the interface.[50] Measurements on laterally confined devices, in which the electrons experience many fewer terraces, showed larger splittings, consistent with expectations from theory,[51,52] and enabling the observation of Pauli spin blockade.[53–57] Spin blockade now has been used to perform single-shot readout and T_1 measurements of singlet-triplet qubits in Si/SiGe.[58,59]

Gating strategies for quantum dot qubits

Making quantum information processing devices is challenging because of the conflict between the need to control accurately the dynamics of the system to perform a sequence of desired operations, on the one hand, and on the other the need to maintain quantum coherence, which requires that the quantum processor not be subject to unwanted external noise and essentially be decoupled from its environment.

The simplest qubit conceptually is the charge qubit, where the two states of the quantum system are formed from two possible locations for one electron in a double quantum dot. Spin plays no role in this qubit. The two states are the lowest energy levels on each side of the double quantum dot, with oscillations between the states caused by introducing a tunnel coupling between the two states. Quantum oscillations of the electron position in charge qubits in superconductors were demonstrated quite early,[60] with charge qubits in single-electron quantum dots demonstrated in 2004.[61] The useful frequency of quantum oscillations of charge qubits is currently limited by the rise time of commercially available pulse generators to $\lesssim$5 GHz, while the decoherence rates away from "sweet spots" (where the difference in energies of the two states is independent of external voltages to the first order)[62] are typically $\gtrsim$5 GHz in both GaAs[63] and Si.[17] Therefore, the quantum coherence of charge qubits is not good enough for them to be plausible candidates for scalable quantum computation.

Loss and DiVincenzo[5] pointed out that spins in semiconductors couple much more weakly to their environment than charges do and proposed to implement qubits using spins of electrons in quantum dots. Starting from that seminal suggestion, several implementations of electrically gated quantum dot spin qubits have been achieved experimentally. Coherence times of spin qubits that are orders of magnitude longer than those of charge qubits have been achieved,[15,16,64] and two-qubit gates have been realized in GaAs quantum dots for single-electron qubits[21] and for singlet-triplet qubits,[16] which consist of the $S_z = 0$ subspace of the states of two electrons in a double quantum dot.[33] However, so far, a full set of high-fidelity gates has not been achieved; situations for which the spin coherence time is long have tended to have slow gate times, so more work is needed to improve the figure of merit.

The impact of materials for top-gated quantum dot qubits

As mentioned previously, qubits have been developed in quantum dots fabricated in both III–V and Group IV heterostructures. Quantum dots formed in GaAs/AlGaAs quantum wells are the most advanced, partly because of the early development of quantum dots in this material (first single-electron dots were fabricated in 2000,[36] compared to 2007 in silicon[37]), and partly because of two advantages compared to silicon: a smaller electronic effective mass (which means that the length scale of the devices can be larger, easing lithography requirements) and essentially perfect lattice matching between GaAs and AlGaAs (which eliminates the need to perfect strain grading to minimize misfit dislocations). The main complication of GaAs is the presence of nuclear spins, which cannot be eliminated, because neither Ga nor As has a spin-zero isotope. The strong coupling between electronic spins and nuclear spins is quasi-static, so that echo[65] and feedback[66] techniques can be used to mitigate these decoherence effects, but they nonetheless make achievement of high-fidelity qubit operations challenging.

A major advantage of silicon and germanium for use in qubits is that they each have an abundant spin zero nuclear isotope, so that isotopic purification would enable the elimination of nuclear spins as a decoherence mechanism. Even in natural-abundance Si, which contains some non-zero nuclear spin isotopes, electron coupling to nuclear spins is orders of magnitude weaker than in GaAs. Si also has much weaker spin-orbit coupling. Together, these two differences lead to longer spin relaxation and coherence times[14,15,67] (for related work in donors in Si, see References 23, 24, and 68).

Figure 3 shows measurements of triplet-to-singlet relaxation times in both GaAs and Si quantum dots. While both times are quite long, this relaxation time is much longer in Si (longer than one second in some regimes). **Figure 4** shows quantum oscillations of singlet-triplet qubits in GaAs[12] and in Si.[15] In this type of measurement, which is performed using fast voltage pulses to the electrostatic gates and readout with spin-to-charge conversion, the oscillations correspond to exchanging the spins in the two dots, so that a state with the left spin up and the right spin down becomes left down and right up. As is clear from the scale of the abscissa, the spin coherence time that governs the decay of these oscillations is much longer in Si than in GaAs because of the lower coupling in Si to nuclear spins; however, the period of the quantum oscillations is also much longer, because the rotation frequency is

https://doi.org/10.1557/mrs.2013.208 Published online by Cambridge University Press

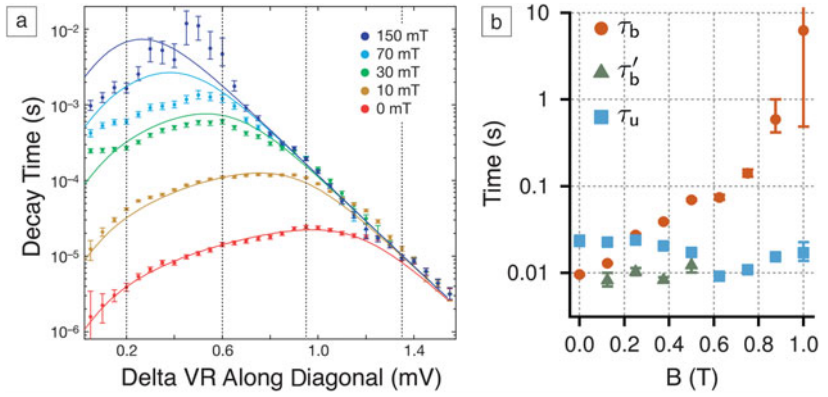


Figure 3. Triplet-singlet relaxation times measured using spin-to-charge conversion in (a) GaAs quantum dots[47] using time-averaged charge sensing (reprinted with permission from Reference 47, © 2005 Macmillan Publishers Ltd.) and in (b) Si quantum dots[58] using single-shot readout (reprinted with permission from Reference 58, © 2012 American Physical Society). Relaxation times are longer in Si qubits because of weaker spin-orbit coupling and weaker coupling between electron spins and nuclear spins.

limited by the size of the magnetic field difference between the two dots, which in these experiments is from the nuclear spins themselves.

Although most work on gated semiconductor quantum dots has been performed with electrons as the charge carriers, holes can also be confined in Si and Ge heterostructures, offering an alternative approach. Hole-based quantum dots have been fabricated in Ge/Si core–shell nanowires,[69] and T_1 relaxation times as long as 0.6 ms have been measured.[70] The g-factor in such devices is expected to be anisotropic, leading to opportunities for optimization based on device and magnetic field orientation.[71] Acceptor-based hole-qubits have been shown theoretically to have strong coherent coupling to phonons, offering a potential route for coupling qubits over distances longer than the size of the hole wave function.[72]

Current work to enhance the fidelity of quantum dot qubits

Several strategies are currently being explored to increase quantum dot qubit fidelities—the degree to which the physical manipulations achieved correspond to the desired outcomes or quantum gates. One challenge to single-spin qubits is the relatively slow speed with which a spin can be flipped using reasonable AC magnetic fields. An alternative approach is to use electric fields to oscillate the electron position rapidly in the presence of either strong spin-orbit coupling or a gradient in the imposed DC magnetic field. GaAs has reasonably strong spin-orbit coupling, and in this material, AC electric fields applied to quantum dots have been shown to rotate single spins.[19] A second approach is to construct qubits in materials with strong spin-orbit coupling, such as InSb nanowires.[73] Qubit operations performed using this method are fast, but decoherence times are short, because spin-orbit coupling also increases the susceptibility to charge fluctuations and electrical noise.

Large gradients in the magnetic field are found near micrometer-sized ferromagnetic materials. Such micromagnets have been fabricated in close proximity to gates defining GaAs quantum dots (Figure 2c–d), enabling the observation of electrically driven spin resonance.[20,74] A magnetic-field difference between two quantum dots is also an essential component of singlet-triplet qubits, and one approach being pursued (but not yet realized) is to incorporate a micromagnet into a singlet-triplet qubit in Si, so that the magnetic-field difference required for qubit manipulation is larger than the fluctuating nuclear fields that cause decoherence.

A different approach is to use logical spin qubits that can be fully manipulated electrically without the need for spin-orbit coupling, magnetic field gradients, or position-dependent g-factors. The first qubit of this type was proposed in Reference 32 and consists of a pair of three-electron states that have the same total spin S and z-component of spin S_z. The key advantage of this logical qubit is that all-electrical manipulation is intrinsically much faster than manipulation that relies (directly or indirectly) on magnetic fields.[38,75–77] Recently, a "hybrid" quantum dot qubit that is particularly well suited for implementation in Si double quantum dots has been proposed.[34,35] This qubit is also a three-electron qubit but is significantly simpler to implement experimentally because it is implemented in a double dot instead of a triplet dot.

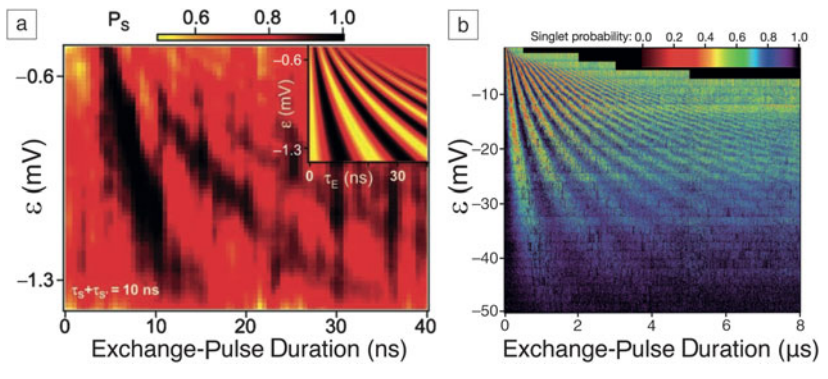


Figure 4. Measurements of quantum oscillations of singlet-triplet qubits, fabricated using double quantum dots in (a) GaAs/AlGaAs[12] (reprinted with permission from Reference 12, © 2005 American Association for the Advancement of Science) and (b) Si/SiGe (reprinted with permission from Reference 15, © 2012 Macmillan Publishers Ltd). The oscillations are between the (↑↓) and (↓↑) states, with rotations induced by the exchange interaction. The decoherence time in the Si qubit (the characteristic time over which the oscillations become less well defined) is hundreds of nanoseconds, compared to tens of nanoseconds in GaAs. However, the oscillation period in Si is also much longer, because the reduction in nuclear fields that leads to the longer spin coherence time also limits the speed of manipulation.

https://doi.org/10.1557/mrs.2013.208 Published online by Cambridge University Press

Logical spin qubits formed from more than one electron often make use of the exchange interaction, providing an attractive combination of fast manipulation speeds and long coherence times between manipulations. However, the coherence time decreases greatly during the manipulation itself, an issue that must be understood and addressed. This enhanced decoherence can be ameliorated by a combination of materials advances (to reduce charge noise) and by qubit design (to reduce the decoherence arising from a given level of charge noise). Work to address this critical issue is of intense current interest.[38]

Summary and outlook

Recent progress in quantum dot-based qubits has been rapid. Hosting qubits in semiconductor materials offers great potential for scalability and synergy with fully integrated classical integrated circuits. One of the exciting features of recent work has been the expansion of the number and variety of quantum dot-based qubits under study, ranging from true spin-1/2 qubits to two- and three-electron logical spin qubits that offer additional flexibility for design and optimization. Improvements in materials, such as high-quality oxides that can be grown or deposited at low temperatures, would enable faster progress for all of these qubits. Reduction in charge noise, though less critical for spin qubits than for charge qubits, will nonetheless be important for the performance of high-speed spin qubit manipulation, which often relies on the electron exchange interaction. These and future advances will offer the prospect of achieving the ultimate goal of the development of a scalable quantum computing architecture.

Acknowledgments

We thank past and current members of the UW–Madison Si/SiGe quantum computing group for years of fruitful collaboration. Research at UW–Madison has been supported, in part, by the Army Research Office (W911NF-08–1-0482, W911NF-12–1-0607), by the National Science Foundation (DMR-0805045, DMR-1206915, PHY-1104660), and by the US Department of Defense. The views and conclusions contained in this document are those of the authors and should not be interpreted as representing the official policies, either expressly or implied, of the US Government. Development and maintenance of the growth facilities used for fabricating samples at UW–Madison is supported by the DOE (DE-FG02–03ER46028).

References

1. P.W. Shor, *SIAM J. Comput.* **26**, 1484 (1997).
2. R.P. Feynman, *Opt. News* **11**, 11 (1985).
3. T. Monz, P. Schindler, J.T. Barreiro, M. Chwalla, D. Nigg, W.A. Coish, M. Harlander, W. Hänsel, M. Hennrich, R. Blatt, *Phys. Rev. Lett.* **106**, 130506 (2011).
4. A.G. Fowler, M. Mariantoni, J.M. Martinis, A.N. Cleland, *Phys. Rev. A* **86**, 032324 (2012).
5. D. Loss, D.P. DiVincenzo, *Phys. Rev. A* **57**, 120 (1998).
6. R. Vrijen, E. Yablonovitch, K. Wang, H.W. Jiang, A. Balandin, V. Roychowdhury, T. Mor, D. DiVincenzo, *Phys. Rev. A*, **62**, 012306 (2000).
7. C. Tahan, M. Friesen, R. Joynt, *Phys. Rev. B* **66**, 035314 (2002).
8. R de Sousa, S. Das Sarma, *Phys. Rev. B* **67**, 033301 (2003).
9. M. Friesen, P. Rugheimer, D.E. Savage, M.G. Lagally, D.W. van der Weide, R. Joynt, M.A. Eriksson, *Phys. Rev. B* **67**, 121301 (2003).
10. W. Witzel, S. Das Sarma, *Phys. Rev. B* **74**, 035322 (2006).
11. A.M. Stephens, A.G. Fowler, L.C.L. Hollenberg, *Quantum Inf. Comput.* **8**, 330 (2008).
12. J.R. Petta, A.C. Johnson, J.M. Taylor, E.A. Laird, A. Yacoby, M.D. Lukin, C.M. Marcus, M.P. Hanson, A.C. Gossard, *Science* **309**, 2180 (2005).
13. F.H.L. Koppens, C. Buizert, K.J. Tielrooij, I.T. Vink, K.C. Nowack, T. Meunier, L.P. Kouwenhoven, L.M.K. Vandersypen, *Nature* **442**, 766 (2006).
14. C.B. Simmons, J.R. Prance, B.J. Van Bael, T.S. Koh, Z. Shi, D.E. Savage, M.G. Lagally, R. Joynt, M. Friesen, S.N. Coppersmith, M.A. Eriksson, *Phys. Rev. Lett.* **106**, 156804 (2011).
15. B.M. Maune, M.G. Borselli, B. Huang, T.D. Ladd, P.W. Deelman, K.S. Holabird, A.A. Kiselev, I. Alvarado-Rodriguez, R.S. Ross, A.E. Schmitz, M. Sokolich, C.A. Watson, M.F. Gyure, A.T. Hunter, *Nature* **481**, 344 (2012).
16. M.D. Shulman, O.E. Dial, S.P. Harvey, H. Bluhm, V. Umansky, A. Yacoby, *Science* **336**, 202 (2012).
17. Z. Shi, C.B. Simmons, D.R. Ward, J.R. Prance, R.T. Mohr, T.S. Koh, J.K. Gamble, X. Wu, D.E. Savage, M.G. Lagally, M. Friesen, S.N. Coppersmith, M.A. Eriksson, *Phys. Rev. B* **88**, 075416 (2013).
18. R. Hanson, L.P. Kouwenhoven, J.R. Petta, S. Tarucha, L.M.K. Vandersypen, *Rev. Mod. Phys.* **79**, 1217 (2007).
19. K.C. Nowack, F.H.L. Koppens, Y.V. Nazarov, L.M.K. Vandersypen, *Science* **318**, 1430 (2007).
20. M. Pioro-Ladrière, T. Obata, Y. Tokura, Y.-S. Shin, T. Kubo, K. Yoshida, T. Taniyama, S. Tarucha, *Nat. Phys.* **4**, 776 (2008).
21. K.C. Nowack, M. Shafiei, M. Laforest, G.E.D.K. Prawiroatmodjo, L.R. Schreiber, C. Reichl, W. Wegscheider, L.M.K. Vandersypen, *Science* **333**, 1269 (2011).
22. B. Kane, *Nature* **393**, 133 (1998).
23. J.J. Pla, K.Y. Tan, J.P. Dehollain, W.H. Lim, J.J.L. Morton, D.N. Jamieson, A.S. Dzurak, A. Morello, *Nature* **489**, 541 (2012).
24. M. Fuechsle, J.A. Miwa, S. Mahapatra, H. Ryu, S. Lee, O. Warschkow, L.C.L. Hollenberg, G. Klimeck, M.Y. Simmons, *Nat. Nanotechnol.* **7**, 242 (2012).
25. F.A. Zwanenburg, A.S. Dzurak, A. Morello, M.Y. Simmons, L.C.L. Hollenberg, G. Klimeck, S. Rogge, S.N. Coppersmith, M.A. Eriksson, *Rev. Mod. Phys.* **85**, 961 (2013).
26. H.L. Störmer, R. Dingle, A.C. Gossard, W. Wiegmann, M.D. Sturge, *Solid State Commun.* **29**, 705 (1979).
27. P. Mooney, *Mater. Sci. Eng., R* **17**, 105 (1996).
28. F. Schäffler, *Semicond. Sci. Technol.* **12**, 1515 (1997).
29. T.M. Lu, D.C. Tsui, C.-H. Lee, C.W. Liu, *Appl. Phys. Lett.* **94**, 182102 (2009).
30. M. Field, C.G. Smith, M. Pepper, D.A. Ritchie, J.E.F. Frost, G.A.C. Jones, D.G. Hasko, *Phys. Rev. Lett.* **70**, 1311 (1993).
31. D. Taubert, M. Pioro-Ladrière, D. Schroeer, D. Harbusch, A.S. Sachrajda, S. Ludwig, *Phys. Rev. Lett.* **100**, 176805 (2008).
32. D.P. DiVincenzo, D. Bacon, J. Kempe, G. Burkard, K.B. Whaley, *Nature* **408**, 339 (2000).
33. J. Levy, *Phys. Rev. Lett.* **89**, 147902 (2002).
34. Z. Shi, C.B. Simmons, J.R. Prance, J.K. Gamble, T.S. Koh, Y.-P. Shim, X. Hu, D.E. Savage, M.G. Lagally, M.A. Eriksson, M. Friesen, S.N. Coppersmith, *Phys. Rev. Lett.* **108**, 140503 (2012).
35. T.S. Koh, J.K. Gamble, M. Friesen, M.A. Eriksson, S.N. Coppersmith, *Phys. Rev. Lett.* **109**, 250503 (2012).
36. M. Ciorga, A.S. Sachrajda, P. Hawrylak, C. Gould, P. Zawadzki, S. Jullian, Y. Feng, Z. Wasilweski, *Phys. Rev. B* **61**, 16315 (2000).
37. C.B. Simmons, M. Thalakulam, N. Shaji, L.J. Klein, H. Qin, R. Blick, D.E. Savage, M.G. Lagally, S.N. Coppersmith, M.A. Eriksson, *Appl. Phys. Lett.* **91**, 213103 (2007).
38. J. Medford, J. Beil, J.M. Taylor, E.I. Rashba, H. Lu, A.C. Gossard, C.M. Marcus, *Phys. Rev. Lett.* **111**, 050501 (2013).
39. R.J. Schoelkopf, P. Wahlgren, A.A. Kozhevnikov, P. Delsing, D.E. Prober, *Science* **280**, 1238 (1998).
40. D.J. Reilly, C.M. Marcus, M.P. Hanson, A.C. Gossard, *Appl. Phys. Lett.* **91**, 162101 (2007).
41. S.J. Angus, A.J. Ferguson, A.S. Dzurak, R.G. Clark, *Appl. Phys. Lett.* **92**, 112103 (2008).
42. T.M. Gurrieri, M.S. Carroll, M.P. Lilly, J.E. Levy, "CMOS Integrated Single Electron Transistor Electrometry (CMOS-SET) Circuit Design for Nanosecond Quantum-Bit Read-out," *NANO'08—8th IEEE Conference on Nanotechnology*, 2008.
43. D.R. Ward, D.E. Savage, M.G. Lagally, S.N. Coppersmith, M.A. Eriksson, *Appl. Phys. Lett.* **102**, 213107 (2013).
44. R. Hanson, B. Witkamp, L.M.K. Vandersypen, L.H. Willems van Beveren, J.M. Elzerman, L.P. Kouwenhoven, *Phys. Rev. Lett.* **91**, 196802 (2003).
45. J.M. Elzerman, R. Hanson, L.H. Willems van Beveren, B. Witkamp, L.M.K. Vandersypen, L.P. Kouwenhoven, *Nature* **430**, 431 (2004).

https://doi.org/10.1557/mrs.2013.208 Published online by Cambridge University Press

46. S. Amasha, K. Maclean, I.P. Radu, D.M. Zumbühl, M.A. Kastner, M.P. Hanson, A.C. Gossard, *Phys. Rev. Lett.* **100**, 046803 (2008).
47. A.C. Johnson, J.R. Petta, J.M. Taylor, A. Yacoby, M.D. Lukin, C.M. Marcus, M.P. Hanson, A.C. Gossard, *Nature* **435**, 925 (2005).
48. K. Ono, D.G. Austing, Y. Tokura, S. Tarucha, *Science* **297**, 1313 (2002).
49. K. Lai, W. Pan, D.C. Tsui, S. Lyon, M. Mühlberger, F. Schäffler, *Phys. Rev. Lett.* **96**, 076805 (2006).
50. S. Goswami, K.A. Slinker, M. Friesen, L.M. McGuire, J.L. Truitt, C. Tahan, L.J. Klein, J.O. Chu, P.M. Mooney, D.W. van der Weide, R. Joynt, S.N. Coppersmith, M.A. Eriksson, *Nat. Phys.* **3**, 41 (2007).
51. M. Friesen, S.N. Coppersmith, *Phys. Rev. B* **81**, 115324 (2010).
52. Z. Jiang, N. Kharche, T. Boykin, G. Klimeck, *Appl. Phys. Lett.* **100**, 103502 (2012).
53. N. Shaji, C.B. Simmons, M. Thalakulam, L.J. Klein, H. Qin, H. Luo, D.E. Savage, M.G. Lagally, A.J. Rimberg, R. Joynt, M. Friesen, R.H. Blick, S.N. Coppersmith, M.A. Eriksson, *Nat. Phys.* **4**, 540 (2008).
54. H.W. Liu, T. Fujisawa, Y. Ono, H. Inokawa, A. Fujiwara, K. Takashina, Y. Hirayama, *Phys. Rev. B* **77**, 073310 (2008).
55. N.S. Lai, W.H. Lim, C.H. Yang, F.A. Zwanenburg, W.A. Coish, F. Qassemi, A. Morello, A.S. Dzurak, *Sci. Rep.* **1**, 110 (2011).
56. Z. Shi, C.B. Simmons, J.R. Prance, J.K. Gamble, M. Friesen, D.E. Savage, M.G. Lagally, S.N. Coppersmith, M.A. Eriksson, *Appl. Phys. Lett.* **99**, 233108 (2011).
57. M.G. Borselli, K. Eng, E.T. Croke, B.M. Maune, B. Huang, R.S. Ross, A.A. Kiselev, P.W. Deelman, I. Alvarado-Rodriguez, A.E. Schmitz, M. Sokolich, K.S. Holabird, R.M. Hazard, M.F. Gyure, A.T. Hunter, *Appl. Phys. Lett.* **99**, 063109 (2011).
58. J.R. Prance, Z. Shi, C.B. Simmons, D.E. Savage, M.G. Lagally, L.R. Schreiber, L.M.K. Vandersypen, M. Friesen, R. Joynt, S.N. Coppersmith, M.A. Eriksson, *Phys. Rev. Lett.* **108**, 046808 (2012).
59. C.H. Yang, A. Rossi, R. Ruskov, N.S. Lai, F.A. Mohiyaddin, S. Lee, C. Tahan, G. Klimeck, A. Morello, A.S. Dzurak, *Nat. Commun.* **4**, 2069 (2013).
60. Y. Nakamura, Y.A. Pashkin, J.S. Tsai, *Nature* **398**, 786 (1999).
61. J.R. Petta, A.C. Johnson, C.M. Marcus, M.P. Hanson, A.C. Gossard, *Phys. Rev. Lett.* **93**, 186802 (2004).
62. D. Vion, A. Aassime, A. Cottet, P. Joyez, H. Pothier, C. Urbina, D. Esteve, M.H. Devoret, *Science* **296**, 886 (2002).
63. K.D. Petersson, J.R. Petta, H. Lu, A.C. Gossard, *Phys. Rev. Lett.* **105**, 246804 (2010).
64. O.E. Dial, M.D. Shulman, S.P. Harvey, H. Bluhm, V. Umansky, A. Yacoby, *Phys. Rev. Lett.* **110**, 146804 (2013).
65. H. Bluhm, S. Foletti, I. Neder, M. Rudner, D. Mahalu, V. Umansky, A. Yacoby, *Nat. Phys.* **7**, 109 (2010).
66. H. Bluhm, S. Foletti, D. Mahalu, V. Umansky, A. Yacoby, *Phys. Rev. Lett.* **105**, 216803 (2010).
67. L.V.C. Assali, H.M. Petrilli, R.B. Capaz, B. Koiller, X. Hu, S. Das Sarma, *Phys. Rev. B* **83**, 165301 (2011).
68. H. Büch, S. Mahapatra, R. Rahman, A. Morello, M.Y. Simmons, *Nat. Commun.* **4**, 2017 (2013).
69. Y. Hu, H.O. Churchill, D.J. Reilly, J. Xiang, C.M. Lieber, C.M. Marcus, *Nat. Nanotechnol.* **2**, 622 (2007).
70. Y. Hu, F. Kuemmeth, C.M. Lieber, C.M. Marcus, *Nat. Nanotechnol.* **7**, 47 (2012).
71. F. Maier, C. Kloeffel, D. Loss, *Phys. Rev. B* **87**, 161305 (2013).
72. O.O. Soykal, R. Ruskov, C. Tahan, *Phys. Rev. Lett.* **107**, 235502 (2011).
73. S. Nadj-Perge, S.M. Frolov, E.P.A.M. Bakkers, L.P. Kouwenhoven, *Nature* **468**, 1084 (2010).
74. T. Takakura, M. Pioro-Ladrière, T. Obata, Y.-S. Shin, R. Brunner, K. Yoshida, T. Taniyama, S. Tarucha, *Appl. Phys. Lett.* **97**, 212104 (2010).
75. E.A. Laird, J.M. Taylor, D.P. Divincenzo, C.M. Marcus, M.P. Hanson, A.C. Gossard, *Phys. Rev. B* **82**, 075403 (2010).
76. G. Granger, L. Gaudreau, A. Kam, M. Pioro-Ladrière, S.A. Studenikin, Z.R. Wasilewski, P. Zawadzki, A.S. Sachrajda, *Phys. Rev. B* **82**, 075304 (2010).
77. L. Gaudreau, G. Granger, A. Kam, G.C. Aers, S.A. Studenikin, P. Zawadzki, M. Pioro-Ladrière, Z.R. Wasilewski, A.S. Sachrajda, *Nat. Phys.* **8**, 54 (2011).
78. L.J. Klein, K.L.M. Lewis, K.A. Slinker, S. Goswami, D.W. van der Weide, R.H. Blick, P.M. Mooney, J.O. Chu, S.N. Coppersmith, M. Friesen, M.A. Eriksson, *J. Appl. Phys.* **99**, 023509 (2006).
79. S.A. Scott, M.G. Lagally, *J. Phys. D.* **40**, 75 (2007).
80. D.M. Paskiewicz, B. Tanto, D.E. Savage, M.G. Lagally, *ACS Nano* **5**, 5814 (2011). □



https://doi.org/10.1557/mrs.2013.208 Published online by Cambridge University Press